

# HIGHER ORDER MODE BEAM BREAKUP LIMITS IN THE SUPERCONDUCTING CAVITIES OF THE SPL

M. Schuh<sup>1,2</sup>, F. Gerigk<sup>1</sup>, J. Tückmantel<sup>1</sup>, C.P. Welsch<sup>3,4</sup>

<sup>1</sup>CERN, Geneva, Switzerland, <sup>2</sup>MPI-K, Heidelberg, Germany,

<sup>3</sup>The University of Liverpool and <sup>4</sup>Cockcroft Institute, Warrington, United Kingdom

## Abstract

The Superconducting Proton Linac (SPL) at CERN is part of the planned injector upgrade of the LHC. Initially used at low duty cycle as LHC injector it has the potential to be upgraded as a high power proton driver for neutrino physics and/or radioactive ion beams.

In this paper the influence of the beam parameters on the build-up of Higher Order Mode (HOM) voltages is studied together with their interaction on the beam. For this purpose we use bunch tracking simulations in the longitudinal and transverse plane in order to define Beam Break-Up (BBU) limits. These simulations take into account changing values for the HOM frequency spread and are carried out using various distances between the HOM frequencies and the main machine lines.

## INTRODUCTION

The High-Power version of the SPL (HP-SPL) [1], [2] is planned as a 4 MW superconducting linac in pulsed operation. Two families ( $\beta_d = 0.65$  and  $\beta_d = 1.0$ ) of 5 cell superconducting elliptical  $\pi$ -mode cavities, in total around 246 (54/192), operating at 704.4 MHz will be used to accelerate  $H^-$  from 160 MeV up to 5 GeV. A maximum pulse length of 1.2 ms is foreseen with an average current up to 40 mA and a repetition rate of 50 Hz.

Reliability of the linac is one of the major design criteria and instabilities caused by HOMs at high beam current are one of the present concerns. Therefore the damping requirements in terms of  $Q_{ex}$  have to be studied carefully in order to provide a high brilliance beam with minimum down time due to quenches in later operation.

In [3] we introduced a code for the analysis of longitudinal beam dynamics in the presence of HOM monopoles. This paper will describe the extension of the code to the transverse plane. The focus is set on dipole modes and their beam interaction.

A point-like bunch of charge  $q$ , passing the cavity off-axis with distance  $x$ , induces a purely imaginary transverse voltage

$$\Delta V_{\perp} = ixq \frac{\omega^2}{c} (R/Q)_{\perp}(\beta) \quad (1)$$

where  $\omega$  is the mode frequency,  $(R/Q)_{\perp}(\beta)$  the effective  $R/Q$  value of this mode at the beam velocity  $\beta c$ . According to the *Panofski-Wenzel theorem* a complex voltage  $V_{\perp}$  yields a transverse momentum kick

$$\Delta p_x = q \frac{\Re(V_{\perp})}{c} \quad (2)$$

which gives rise to a transverse velocity change (for small angles) of

$$\Delta x' = \Delta p_x / p_{\parallel} = q \frac{\Re(V_{\perp})}{cp_{\parallel}} \quad (3)$$

where  $p_{\parallel}$  is the longitudinal momentum and  $\Re(V_{\perp})$  the real part of the HOM voltage. There is no direct interaction between the voltage induced by a bunch and the bunch itself since there is a phase difference of  $90^\circ$  between them. If a pulse with several bunches passes a cavity, one has to sum up the induced voltage taking into account their phase relationship and their exponential decay with a time constant of  $T_d = \frac{2Q_{ex}}{\omega_n}$ . The transverse focusing is assumed to be smooth and is applied in the inter cavity drift space using  $2 \times 2$  transfer matrices.

We compare the phase space areas at the end of the linac created by all bunches in a pulse to measure the impact of HOMs. The effective emittance  $\epsilon$  is defined as

$$\epsilon = \pi \sqrt{\langle x^2 \rangle \langle x'^2 \rangle - \langle xx' \rangle^2} \quad (4)$$

and the emittance growth rate is then defined as the effective emittance ratio of (HOM-) disturbed bunches over undisturbed bunches. A bunch is defined as lost, if the transverse displacement is larger than the cavity iris.

## SIMULATION PARAMETER

In all transverse beam dynamics simulations presented in this paper the following basic assumptions and simplifications are made:

- no alignment errors in the focusing elements;
- all cavities have zero transverse displacement;
- the beam is injected on axis with a normal distributed spread in position ( $\sigma_x = 0.3$  mm) and transverse momentum ( $\sigma_{x'} = 0.3$  mrad);
- one dipole mode per cavity;
- longitudinally matched beam, no HOM monopoles;
- all errors are Gaussian distributed.

All simulations are done with synchronous bunches in the longitudinal plane. The HOM is excited by the beam input noise (bunch charge jitter, input position and momentum spread). The variation of these parameters have a strong influence on building critical HOM voltages and where redefined at a recent SPL HOM workshop [6]. The important figures of each HOM are its frequency, the cavity to cavity HOM frequency spread, and the  $R/Q_{\perp}(\beta)$  map.

### Simulation Input Parameter Review

One of the SPL HOM workshop goals was a critical review of the simulation input parameters. It became clear that the assumed input parameters were too pessimistic, especially the HOM frequency scatter and the bunch charge jitter. In case of the HOM frequency scatter measurements from SNS, TESLA and JLAB are summarized in Table 1. Based on these data the HOM frequency scatter in SPL cavities is now estimated at  $\sigma = 1$  MHz instead of  $\sigma = 0.1$  MHz.

Table 1: HOM Frequency Scatter of Different Cavities and their Operation Frequency

Cavity	$f_{op}$ [MHz]	$\sigma(f_{HOM})$ [MHz]
SNS	805	1 - 4
TESLA (DESY)	1300	1 - 10
CEBAF (JLAB)	1497	0.3- 30

Measurements at SNS [7] show a bunch charge fluctuation of  $\sigma = 0.3\%$ . The results of these measurements lead to the conclusion that a bunch charge jitter of 1% - 3% is a more realistic input parameter than 10% previously assumed. Also a  $\beta$ -dependent  $R/Q$  instead of a constant value should be used in order to avoid an overestimation. Besides the simulation input parameters several effects were identified which might cause problems and have to be investigated. One of these is the influence of a chopped beam which is studied in this contribution together with the  $\beta$ -dependent  $R/Q_{\perp}$ .

Table 2: Revised Simulation Input Parameters - Old Values in Brackets.

Parameter	Value	$\sigma$
$I_{beam}$ [A]	0.04-0.4	3% (10%)
$f_{HOM}$ [MHz]	1015 / 915	1.0 (0.1)
$R/Q_{\perp}$ [ $\Omega$ ]	$R/Q_{\perp}(\beta)$ (60/70)	-

### Emittance Blow-up

The modified input parameters had a major effect on the beam dynamic simulation. All results presented in [3] and [6] showed a dramatic emittance growth rate. There the emittance increased by a factor 100 in some setups and even beam losses were observed. Applying the revised input parameters (see Tab. 2), but still using constant  $R/Q$  values, the longitudinal (Fig. 1) and transverse (Fig. 2) emittance growth rate shrinks to a moderate level. In Fig 1 and 2 the general behaviour does not change compared to the previous results, only the amplitude. Taking also the change of  $R/Q$  with  $\beta$  into account the emittance shrinks further, but only by a small amount.

## 11 High current issues and beam dynamics

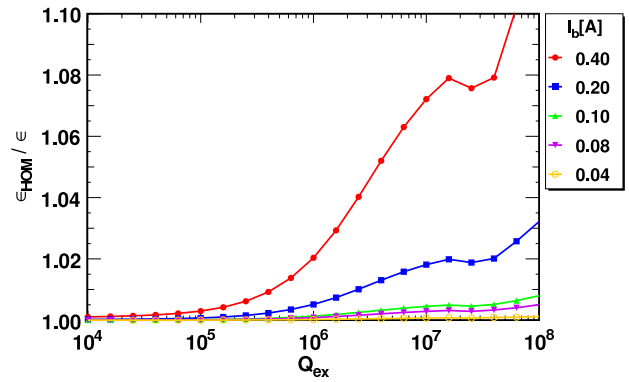


Figure 1: Longitudinal emittance growth rate of the beam against  $Q_{ex}$  with revised input parameters and const.  $R/Q$ .

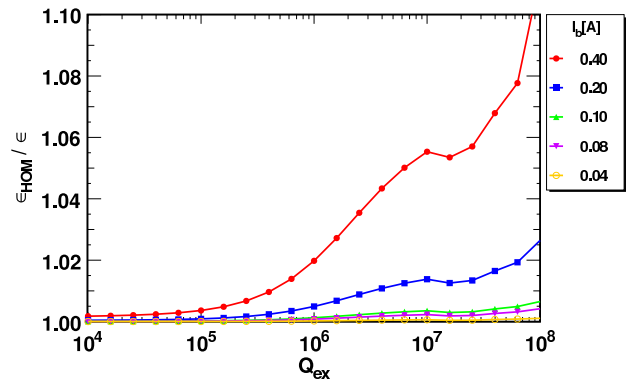


Figure 2: Transverse emittance growth rate of the beam against  $Q_{ex}$  with revised input parameters and const.  $R/Q_{\perp}$ .

### $R/Q_{\perp}(\beta)$ Analysis

One of the cavity parameters needed in the simulation is the  $R/Q_{\perp}$  value for each dipole mode in each cavity. Since the particle velocity changes significantly along the linac (in total from  $\beta = 0.52$  to  $\beta = 0.98$ ) also the effective  $R/Q_{\perp}(\beta)$  changes and is given by

$$R/Q_{\perp}(\beta) = \frac{\int_0^L E_z(\rho = r) e^{i\omega_n z c/\beta} dz}{(r\omega_n/c)^2 \omega_n U_n} \quad [\Omega] \quad (5)$$

where  $L$  is the cavity length,  $U$  the stored energy of the mode with an angular frequency  $\omega_n$ , and the field is integrated parallel to the beam axis with distance  $r$  using the average particle velocity in each cavity. The result is normalized to the unit linac Ohm, which is needed in the simulation code.

In Figure 3 and 4 the typical change of  $R/Q_{\perp}$  with  $\beta$  is shown for two modes in each section. The analysis is done for all relevant dipole modes in the preliminary cavity geometry up to 3 GHz and the results show variations per mode by more than four orders of magnitude. The  $R/Q_{\perp}$  values of the modes at the design  $\beta$  of the cavities are plotted with dashed lines. Figure 3 and 4 show that the  $\beta$  dependence of  $R/Q_{\perp}$  must be included for realistic sim-

ulations. In Table 3 the dipole modes with highest  $R/Q_{\perp}$  values are listed for both cavities.

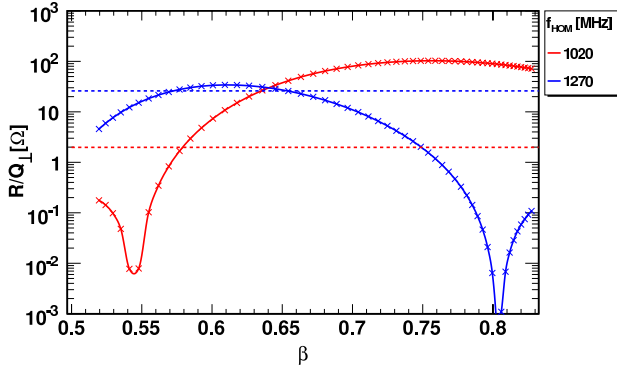


Figure 3:  $R/Q_{\perp}(\beta)$  of two dipole modes along the medium  $\beta$  section. The dashed lines are the  $R/Q_{\perp}$  value at the design  $\beta$  of the cavity.

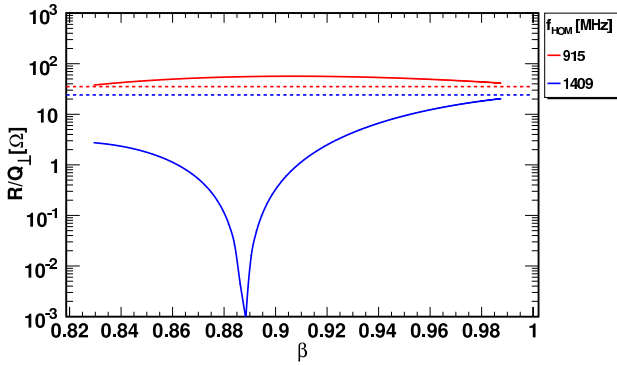


Figure 4:  $R/Q_{\perp}(\beta)$  of two dipole modes along the high  $\beta$  section. The dashed lines are the  $R/Q_{\perp}$  value at the design  $\beta$  of the cavity.

Table 3:  $R/Q_{\perp}$  Values of Dipole Modes in 704 MHz  $\beta_d = 0.65$  and  $\beta_d = 1.0$  Cavity

No	$\beta_d$	$f$ [MHz]	$R/Q_{\perp}$ [ $\Omega$ ] <sup>†</sup>		
			$\beta_d$	max.	avg.
1	0.65	1015	2	143	49
2	0.65	1020	39	107	60
3	0.65	1027	55	57	19
4	0.65	1033	11	30	12
5	0.65	1270	26	34	10
6	1.0	915	35	57	48
7	1.0	940	67	60	44
8	1.0	1014	37	36	27
9	1.0	1020	12	25	20
10	1.0	1409	24	20	12

<sup>†</sup> linac definition

## TRANSVERSE SIMULATIONS

In this section the effect of different HOM frequencies and  $R/Q_{\perp}(\beta)$  maps are studied. All simulations are done

### 11 High current issues and beam dynamics

with the revised input parameters and a beam current of 400 mA (10 times nominal).  $Q_{ex}$  sweeps from  $10^4$  up to  $10^8$ . In order to neglect the influence of the HOM frequency distribution along the linac a so-called default HOM frequency pattern is defined<sup>1</sup>. This will be used in all simulations. The same is done for the input bunch pattern, where the bunch to bunch charge, position and momentum distribution is fixed. Both together are used as default pattern set in all simulations.

Five different HOM setups are used for the study:

1. In each cavity the mode with the highest  $R/Q_{\perp}(\beta)$  value at this beam  $\beta$  is used ( $35\Omega < R/Q_{\perp} < 150\Omega$ ).
2. In both sections the mode sits at the 3rd fundamental machine line (1056.60 MHz),  $R/Q_{\perp}(\beta)$  maps of mode 2 and 6 (see. Tab. 3) are used.
3. Mode 2 and 6 (see. Tab. 3) are used.
4. Mode 5 and 10 (see. Tab. 3) are used.
5. In both sections the mode sits at the 8th fundamental machine line (2817.60 MHz),  $R/Q_{\perp}(\beta)$  maps of modes in this frequency area with the highest  $R/Q_{\perp,avg} \sim 0.2\Omega$  are used.

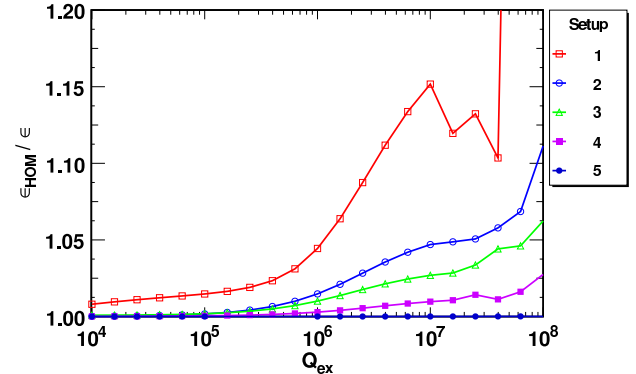


Figure 5: Transverse emittance growth rate of the beam against  $Q_{ex}$  with different dipole mode setups.

Results of all setups are plotted together in Figure 5. From the graph we can see that the first setup has the strongest influence at the beam. In this case not all cavities have the same mean HOM frequency, but very high  $R/Q_{\perp}$  values. The emittance growth rate decreases at around  $Q_{ex} = 2 \cdot 10^7$  which is a behaviour of the used HOM frequency pattern. Repeating the simulations with different patterns a "less spiky" emittance growth is observed. If a HOM falls on a machine line, it has a significant influence, which we can clearly see in setup 2 compared with 3. With decreasing  $R/Q_{\perp}$  the emittance growth decreases rapidly which is illustrated in cases 4 and 5. Increasing the HOM frequency and sitting directly on a machine line has no significant effect, because at the same time  $R/Q_{\perp}$  decreases

<sup>1</sup>The seeds for all random number generators are kept constant and all generators are reset at each simulation step.

(more than quadratic) and therefore also the induced voltage per bunch.

To ensure that the used default beam and HOM frequency pattern is not just an exotic one, chosen by accident, we did statistical simulations with different patterns. Therefore HOM setup 2 with a  $Q_{ex} = 10^7$  and a beam current of 400 mA was chosen. Three different runs were performed where the following was varied:

- HOM frequency pattern
- beam pattern
- a) + b)

The results are illustrated in Figure 6, where also the output distribution of b) without HOM interaction is plotted (left peak). All curves show a Gaussian distribution and no significant differences were found between the three runs. The emittance growth value of the default set is inside the one  $\sigma$  area of two out of the three runs. This leads to the conclusion that the chosen HOM frequency pattern and beam pattern can be used as a representative input set.

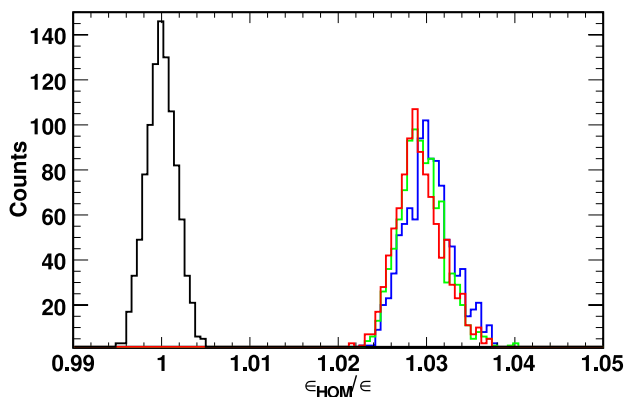


Figure 6: Histogram of the transverse emittance growth rate distribution at  $Q_{ex} = 10^7$  for 1000 setups: a) green, b) blue, c) red. The beam pattern distribution without HOMs is also plotted (left).

In Figure 7 the average (black) and maximum (red) HOM voltage after two pulses is shown. The same parameters are used as in the statistical setup (solid lines). In average an oscillation was observed along the linac. In addition the same simulation was done using a different set of dipole modes (dashed lines - mode 5 and 10 from Tab. 3, plotted in Fig. 3.4). The deep drops in the HOM voltage matches perfectly with the drops in the  $R/Q_{\perp}(\beta)$  map.

## INFLUENCE OF CHOPPING

For the HP-SPL several chopping scenarios are under discussion. The additional chopping time structure introduces new machine lines beside the existing ones at 352.2 MHz and 50 Hz. These frequencies are difficult to

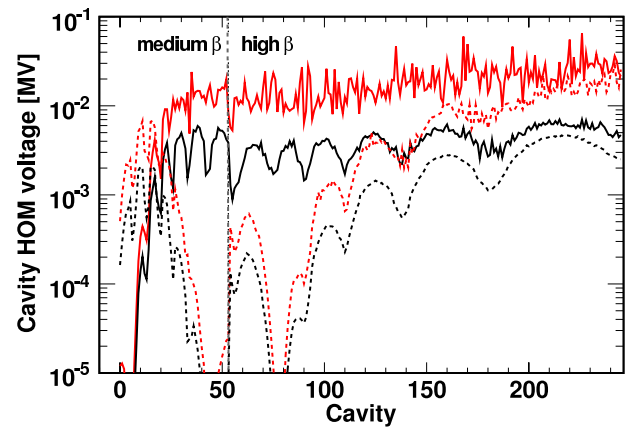


Figure 7: Observed average (black) and maximum (red) HOM voltage distribution along the linac from 1000 different HOM frequency pattern for HOM setup 2 (solid) and 5 (dashed).

anticipate during the cavity design phase, since they depend on the chopping schemes chosen for future applications. However, the general influence of chopping on the HOM build-up and the beam has to be studied and understood in order to identify potential bottle necks early in the design phase.

A case study approach with three different chopping modes (2-4) listed in Table 4 was chosen to allow a general estimation of this effect. The first mode is the unchopped beam, which is used as reference for the remaining analysis. In the second mode 3 bunches out of 8 are chopped. This ratio stays constant, but the number of bunches is multiplied by 10 to 100 for mode 3 and 4. The charge per pulse stays the same as for the unchopped pulse raising the peak current by a factor of 8/5. For this analysis the  $R/Q_{\perp}(\beta)$  maps of modes 2 and 6 (see Tab. 3) are chosen. The frequency of these modes (1020 MHz/915 MHz) is used in the initial setup and then in the second setup (*ML*) shifted to a machine line created by the chopping (see. Tab. 4). Then in both sections the same HOM frequency is applied to have a worst case excitation. An average beam current of 400 mA is used in all simulations which is 10 times the nominal one. All other simulation parameters stay the same which means a HOM frequency spread of 1 MHz, a charge jitter of 3% and the nominal beam input phase space distribution are used. In total 100 linacs were simulated using always the same beam pattern.

The results are illustrated in Figure 8, where the average emittance growth rate is plotted against  $Q_{ex}$ . In chopping mode 3 also the standard deviation is indicated by error bars. It is apparent from this plot that chopping increases the emittance in comparison to the nominal case. There is only a minor difference between the three chopping modes and they all stay inside a  $\pm\sigma$  area. This leads to the conclusion that the peak current is one of the important figures in this effect. Chopping increases the emittance by about the same factor than shifting the HOM frequency to a machine

Table 4: Different Chopping Modes and Used Resonance Frequency (Machine Line).

Mode	chopping	$f_{ML}$ [MHz]
1	no chopping	1056.60
2	5/8	1012.58
3	50/80	1016.98
4	500/800	1018.30

line in the reference setup. If the HOM then falls on a machine line created by the chopping an additional emittance growth is observed. Again, there is no significant difference between the applied chopping modes. Looking at the  $Q_{ex}$  dependency the same general behaviour as in the reference setup is observed. For transverse effects including chopping  $Q_{ex}$  should not exceed  $10^7$ .

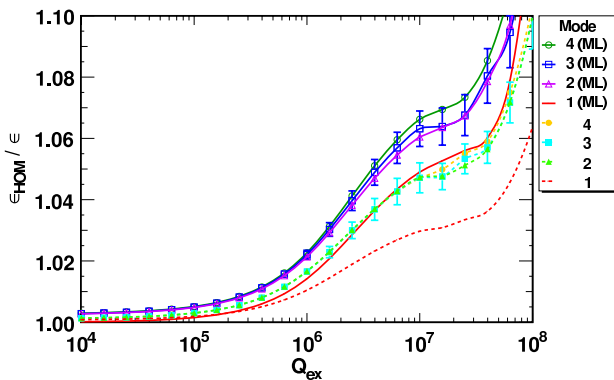


Figure 8: Average transverse emittance growth rate of the beam in 100 linacs against  $Q_{ex}$  for the 4 different chopping modes listed in Tab. 4 with ten times the nominal beam current - mode 3 also error bars ( $\sigma$ ) plotted. The solid lines correspond to a resonance excitation and the dashed ones are off resonance.

An analytic study of power dissipation in HOMs with a sub-structured pulsed beam was reported in [4]. Applying the SPL parameters to these formulae leads to the result that chopping is no major concern as long as  $Q_{ex}$  does not exceed  $10^7$ .

## CODE BENCHMARK

At the SPL HOM Workshop [6] several quite different simulation results produced with different codes were presented. Since most of the codes are based on [5] there should be no deviation between these. In order to classify the different results, the codes were benchmarked against each other. A dedicated test scenario was defined and the output of the codes provided by [9], [10] was compared bunch by bunch against our code and [5]. It could be confirmed that all codes produce the same output within the

### 11 High current issues and beam dynamics

numerical resolution. Details presently under further investigation are to be published.

## CONCLUSION & OUTLOOK

One of the significant findings to emerge from this study is that the review of the simulation input parameter led to significant change in the simulated emittance growth. It has been pointed out that chopping causes an additional transverse emittance growth, however it was found to be within tolerable limits.

In this investigation, the aim was to define upper limits for the damping requirements. Even when using ten times the design current simulation results in the transverse plane showed that a  $Q_{ex}$  of  $10^6 - 10^7$  is acceptable.

Future studies will concentrate on analysing the effects of chopping on the longitudinal plane and of alignment errors in both planes.

## REFERENCES

- [1] O. Brunner et al., "Assessment of the basic parameters of the CERN Superconducting Proton Linac", Phys. Rev. ST Accel. Beams 12, 070402 (2009).
- [2] R. Garoby et al., "SPL", This conference.
- [3] F. Gerigk et al., "Higher Order Modes in the Superconducting Cavities of the SPL", in Proceeding of the Particle Accelerator Conference (PAC09), Vancouver, 2009.
- [4] S. Kim et al., Higher-order-mode (HOM) power in elliptical superconducting cavities for intense pulsed proton accelerators, Nucl. Instr. A 495 (2002) 8594.
- [5] J. Tückmantel, "HOM Dampers or not in Superconducting RF Proton Linacs", BE-Note-2009-009 RF.
- [6] A. Lombardi et al., "Summary of the workshop on HOM in SPL, held at CERN June 25-26.", CERN-sLHC-Project-Note-0003.
- [7] D. A. Bartkoski et al., "High-dynamic-range current measurements in the medium-energy beta transport line at the spallation neutron source", in Proceedings of the Linear Accelerator Conference (LINAC06), Knoxville, 2006.
- [8] D. Jeon et al., "Cumulative beam break-up study of the spallation neutron source superconducting linac", Nuc. Instr. A (2002) 495.
- [9] J.-L. Biarrotte, priv. communication.
- [10] Dobrin Kaltchev, priv. communication.